

Polarization of Protons from the $\text{He}^3(d,p)\text{He}^4$ Reaction*

R. I. BROWN AND W. HAEBERLI
University of Wisconsin, Madison, Wisconsin
 (Received 15 August 1962)

The polarization of protons from the $\text{He}^3(d,p)\text{He}^4$ reaction has been measured at eight laboratory angles between 20° and 140° for six deuteron energies from 3 to 12 MeV. The polarization was determined by scattering the protons from carbon. For all energies measured the polarization is positive at forward angles with a maximum near a laboratory angle of 30° . The polarization passes through zero in the vicinity of 60° and has a broad peak of negative polarization at back angles. At the forward maximum the polarization increases with bombarding energy from $+0.10 \pm 0.03$ at 3 MeV, to $+0.76 \pm 0.03$ at 10 MeV and $+0.73 \pm 0.04$ at 12 MeV. The broad minimum in the polarization at larger angles shows a similar energy dependence but the minimum also shifts to larger angles with increasing deuteron energy. The most negative value of the polarization ($P = -0.66 \pm 0.05$) was found at 120° and 8 MeV. The present measurements suggest that the $\text{He}^3(d,p)\text{He}^4$ reaction may be a useful source of 23–29 MeV polarized protons. The results are compared with measurements of the neutron polarization in the mirror reaction $\text{T}(d,n)\text{He}^4$. Some new information on the polarization in the scattering of protons from carbon has also been obtained.

I. INTRODUCTION

CROSS-SECTION measurements for the $\text{He}^3(d,p)\text{He}^4$ reaction have been reported^{1–5} for deuteron energies from 40 keV to 13.7 MeV. Likewise for the mirror reaction $\text{T}(d,n)\text{He}^4$ several investigations^{4–7} have been carried out. A satisfactory theoretical description of the reactions has not been made except for very low deuteron energies where the cross sections can be described in terms of a resonance forming He^5 or Li^5 in a state of total angular momentum $3/2^+$. The resonance occurs at a deuteron energy of 107 keV for the $\text{T}(d,n)\text{He}^4$ reaction and 430 keV for the $\text{He}^3(d,p)\text{He}^4$ reaction. However, for both reactions deviations from the single level prediction begin a few hundred keV above the resonance. Neither reaction exhibits any further resonances. Only a slight hump in the cross section is observed between $E_d = 3$ and 9 MeV.⁵ At the higher energies the reaction cross section can be compared to calculations based on deuteron stripping theory. (See Sec. V.)

The similarity of the absolute magnitude and angular dependence of the cross section for these two reactions has been pointed out repeatedly.^{3,5,6} This similarity is expected on the basis of charge symmetry of nuclear forces. Likewise the proton polarization in the $\text{He}^3(d,p)\text{He}^4$ reaction should, except for small Coulomb effects, be equal to the neutron polarization in the $\text{T}(d,n)\text{He}^4$

reaction. The work presented in this paper is the first measurement of the proton polarization in the $\text{He}^3(d,p)\text{He}^4$ reaction. Preliminary results were reported⁸ some time ago. Measurements^{9,10} of the neutron polarization in the $\text{T}(d,n)\text{He}^4$ reaction have recently also been made. In earlier experiments^{11,12} with deuteron energies up to 1.8 MeV little or no polarization had been found.

II. APPARATUS

1. General Description

The apparatus is shown in Figs. 1 and 2. Deuterons impinged on a He^3 -filled gas target *A* (Fig. 2) which was positioned in the center of a vacuum chamber *B*. Reaction protons could emerge from the chamber through foil covered windows *C*. The polarization analyzer *D* consisted of a carbon target and two scintillation counters *E* which detected protons scattered 45° to the left and right of the incident protons. For some of the measurements thin scintillators *K* were used in coincidence with the other counters in order to reduce background.

2. Reaction Chamber and He^3 Target

The beam entered the reaction chamber *B* through two pair of slits which formed a rectangular aperture with a horizontal opening of 0.16 cm and a vertical opening of 0.32 cm. The beam current striking the slits was monitored to ascertain that the beam passed symmetrically through the aperture. To make certain that the beam passed through the axis of the chamber the beam position was adjusted such that the beam current was equally divided between the two closely spaced rear

* Work supported by the U. S. Atomic Energy Commission and the Graduate School with funds supplied by the Wisconsin Alumni Research Foundation.

¹ J. Hatton and G. Preston, *Nature* **164**, 145 (1949).

² J. L. Yarnell, R. H. Lovberg, and W. R. Stratton, *Phys. Rev.* **90**, 292 (1953).

³ W. E. Kunz, *Phys. Rev.* **97**, 456 (1955).

⁴ W. R. Arnold, J. A. Phillips, G. A. Sawyer, E. J. Stovall, Jr., and J. L. Tuck, *Phys. Rev.* **93**, 483 (1954).

⁵ L. Steward, J. E. Brolley, Jr., and L. Rosen, *Phys. Rev.* **119**, 1649 (1960).

⁶ M. D. Goldberg and J. M. LeBlanc, *Phys. Rev.* **122**, 164 (1961).

⁷ J. E. Brolley, Jr., and J. L. Fowler, in *Fast Neutron Physics*, edited by J. B. Marion and J. L. Fowler (Interscience Publishers Inc., New York, 1960), Vol. I, Chap. IC, p. 73, give a summary of earlier work.

⁸ R. I. Brown, and W. Haeberli, *Bull. Am. Phys. Soc.* **6**, 307 (1961).

⁹ R. B. Perkins and J. E. Simmons, *Phys. Rev.* **124**, 1153 (1961).

¹⁰ W. Benenson, R. L. Walter, and T. H. May, *Phys. Rev. Letters* **8**, 66 (1962).

¹¹ I. I. Levintov, A. V. Miller, and V. N. Shamshev, *Zh. Eksperim. i Teor. Fiz.* **34**, 1030 (1958) [translation: *Soviet Phys.—JETP* **7**, 712 (1958)].

¹² P. J. Pasma, *Nucl. Phys.* **6**, 141 (1958).

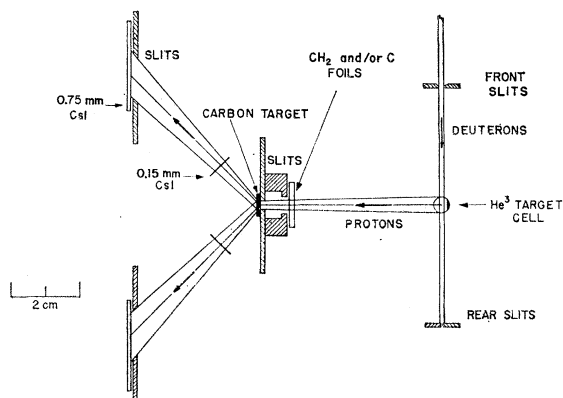


FIG. 1. Schematic of the experimental arrangement.

slits *G* (Fig. 2). The separation of these slits was 0.02 cm. The current of the rear slits was integrated to monitor the duration of the runs. The beam passing through the slits hit a beam stop. The beam stop as well as the slits were made of tantalum.

The chamber had windows every 10° from 10° to 140° for left and right scattering angles. The windows were covered by $2.6\text{-}\mu$ -thick spring steel or nickel foils. The proton energy loss in these foils was at most 60 keV.

The He^3 target consisted of a 0.5-cm outside diam stainless steel tube with 0.08-cm walls which had a window section removed. The window covered an angular range of about 290° . The cylinder was sealed at one end and attached to a flange on the other. "Havar"¹³ foil $2.6\text{ }\mu$ thick was wrapped around the window section and glued with an epoxy resin.¹⁴

The target cells held up to 26 atm of pressure. A target pressure of 17 atm of He^3 was used during the experiment. The target thickness was then 100 to 300 keV. The target cells withstood a total of 0.6 W of beam heating in the gas and in the entrance and exit spots on the foil. This corresponds to $0.7\text{ }\mu\text{A}$ of deuterons at 3 MeV or $1.9\text{ }\mu\text{A}$ at 12 MeV. The foils were not entirely leak tight. In some cases the loss was less than 5% during a 48-h run. It was necessary, however, to avoid a tightly focused beam since the resulting hot spot on the foil allows the helium to diffuse rapidly out of the cell.

In order to compress the He^3 into the target cell a simple pump consisting of a balloon inside a compression chamber was used. The pump is described in detail elsewhere.¹⁵

3. Carbon Analyzer

The carbon analyzer is shown in Figs. 1 and 2. Because of the high Q value of the $\text{He}^3(d,p)\text{He}^4$ reaction

($Q=18.4$ MeV) a simple design was possible: The protons traveled in air and relatively thick, sturdy carbon targets could be used.

The entrance slit to the analyzer was 0.25 cm wide and 0.76 cm high. Directly behind it was inserted the carbon target at a distance of 5.0 cm from the center of the He^3 target. A rectangular aperture 1.4 cm wide and 1.9 cm high defined the acceptance area for the detectors. The centers of the detectors were 5.0 cm from the carbon target and were placed at 45° to the right and to the left of the protons incident on the carbon. The analyzer was mounted on a heavy steel ring (*H* in Fig. 2) which rotated about the vacuum chamber. A ground surface bar *J* was attached to the ring to provide reproducible positioning for the analyzer.

Targets of high-purity graphite were used. The thicknesses varied from 27 to 114 mg/cm^2 . For the proton energies involved this corresponded to an energy loss of 1 to 3 MeV. Cesium iodide crystals 0.08 cm thick were used as detectors. The proton energy at detection ranged from 9 to 14 MeV for the different angles at which measurements were made. For the higher energies, steel foil was placed in front of the detectors to insure that the protons were stopped in the crystals.

A set of polyethylene foils from 0.0025 to 0.05 cm thick and several thin slabs of graphite were used to slow the protons incident on the carbon analyzer to the desired energy. The holder for the slowing-down foils also served as an antiscattering baffle, i.e., it assured that no protons scattered in the windows of the scattering chamber could by direct flight reach the detectors.

Calculations for beam divergence due to multiple scattering in the slowing-down foils were made from the Molière theory in the manner described by Bichsel.¹⁶

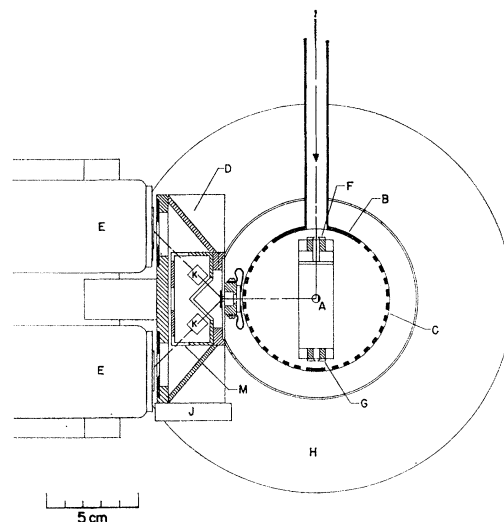


FIG. 2. Top view of reaction chamber and carbon analyzer. *A*, He^3 target cell; *B*, reaction chamber; *C*, windows; *D*, polarization analyzer; *E*, phototubes with CsI crystals; *F*, beam front slits; *G*, beam rear slits; *H*, rotating ring mount; *J*, alignment bar; *K*, thin CsI crystals; *M*, coincidence telescope box.

¹³ Havar is the trade name of Hamilton Watch Company, Lancaster, Pennsylvania, for a high tensile strength spring steel alloy.

¹⁴ Armstrong A-4, Armstrong Products, Warsaw, Indiana.

¹⁵ R. I. Brown, Ph.D. thesis, University of Wisconsin, 1961. Available through University Microfilms, Ann Arbor, Michigan.

¹⁶ H. Bichsel, Phys. Rev. **112**, 182 (1958).

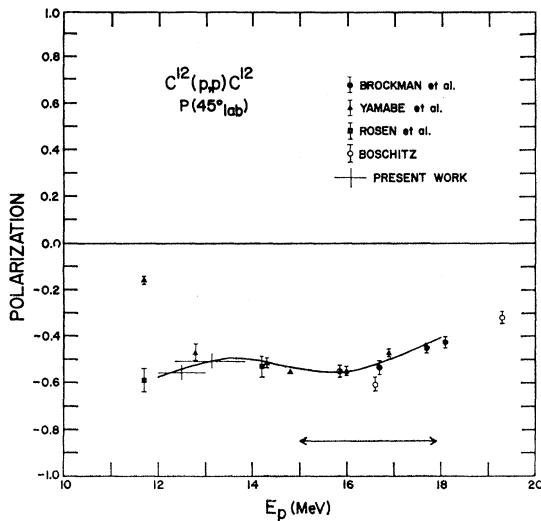


FIG. 3. Analyzing power of carbon for proton elastic scattering. The points are those of Brockman, Yamabe, Rosen, and Boschitz (see references 19, 17, 18, and 20, respectively) for scattering through a laboratory angle of 45° . The target thickness for these measurements was about 1 MeV. The solid curve is the weighted mean of the analyzing power for the analyzer used in the present experiment. The line at the bottom of the figure indicates the energy spread in the most frequently used carbon target.

In the extreme case that 30-MeV protons were slowed to 18 MeV, the mean angular spread in the proton beam due to multiple scattering was $\pm 4^\circ$.

4. Coincidence Counter Telescope

For the measurements at 10 and 12 MeV it was necessary to add a coincidence detector to the analyzer in order to reduce background. Two CsI crystals (K in Fig. 2) 0.15 mm thick were mounted in the analyzer to intersect the scattered protons. Consequently, coincident signals were produced by protons in the thick and thin crystals.

The normal to each of the thin crystals made a 30° angle with respect to the incident protons. This allowed both thin crystals to be viewed from above by the photocathode of a single phototube. The thin crystals were mounted in a separate light-tight aluminum box (M of Fig. 1) which was inserted between the front and rear slits of the analyzer. Thin nickel foils provided windows for the entrance and exit of the protons.

III. PROCEDURE

1. Analyzing Power of Carbon

In order to obtain the proton polarization P_1 from the measured left-right asymmetries it is necessary to know the analyzing power P_2 of carbon. Since P_2 depends on scattering angle and on energy, the effective analyzing power $P_{2,\text{eff}}$ is the mean of $P_2(E_p, \theta)$ over the angular acceptance of the analyzer and over the energy spread of protons scattered in the carbon target. The average of P_2 with respect to angle, $\langle P_2(\theta) \rangle_{\text{av}}$, was cal-

culated using previous measurements of $P(\theta)$ near 14 MeV,^{17,18} near 16 MeV,^{17,19,20} and at 17.7 MeV.¹⁹ The weight assigned to $P_2(\theta)$ was proportional to $f(\theta) \times \sigma(\theta)$, where $f(\theta)$ is the differential acceptance solid angle of the analyzer as a function of the laboratory angle θ and $\sigma(\theta)$ is the differential scattering cross section of carbon. In computing $f(\theta)$ the effect of the finite height of the slits was also taken into account. The function $f(\theta)$ was found to resemble a Gaussian with a mean angle of 46° and a rms spread of $\pm 4^\circ$. For $\sigma(\theta)$ the measurements of Peelle²¹ and of Nagahara²² were used.

At several other energies measurements of $P_2(45^\circ)$ were available.¹⁷⁻²⁰ At these energies $\langle P_2(\theta) \rangle_{\text{av}}$ was obtained by assuming that the angular dependence of P_2 is similar to that at neighboring energies where $P(\theta)$ had been measured. The solid line in Fig. 3 represents $\langle P_2(\theta) \rangle_{\text{av}}$ as a function of proton energy. The points show the various measurements of $P(45^\circ)$ on which the calculations were based. The values of the effective analyzing power $P_{2,\text{eff}}$ were then obtained by averaging the curve of Fig. 3 over the energy spread of the protons in the target. The range of proton energies in the most frequently used carbon target is indicated by a line at the bottom of Fig. 3.

The above calculation neglected the fact that P_2 should further be multiplied by a factor $\cos\phi$, where ϕ is the azimuthal angle. The vertical extent of the slits caused an extreme spread in azimuthal angle of 18° which leads to a mean value of $\cos\phi$ of 0.976.

As can be seen in Fig. 3 there is considerable disagreement in the experimental data for $P_2(45^\circ)$ at 11.7 MeV. This region was, therefore, avoided as much as possible. However, since the proton energy from the $\text{He}^3(d,p)\text{He}^4$ reaction at a laboratory angle of 140° is as low as 13 MeV it was necessary to use the 12- to 13-MeV region for measurements at that angle. For this reason the analyzing power of carbon between 12 and 14 MeV was

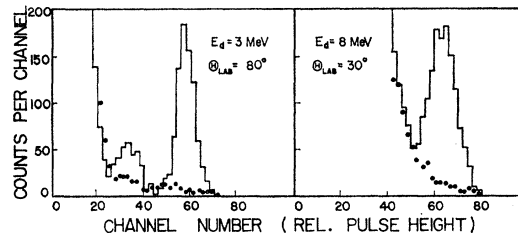


FIG. 4. Pulse-height spectra of the $\text{He}^3(d,p)$ protons scattered from carbon at 45° for deuteron energies of 3 and 8 MeV. The dots show the spectra when the carbon target was removed. In the 3-MeV spectrum one observes peaks corresponding to elastic and inelastic scattering of protons from carbon. In the 8-MeV spectrum the inelastic peak is masked by background.

¹⁷ S. Yamabe, M. Kondo, S. Kato, T. Yamazaki, and J. Ruan, *J. Phys. Soc. Japan* **15**, 2154 (1960).

¹⁸ L. Rosen, P. Darriulat, H. Faraggi, and A. Garin, *Nucl. Phys.* **33**, 458 (1962).

¹⁹ K. W. Brockman, Jr., *Phys. Rev.* **110**, 163 (1958).

²⁰ E. Boschitz, *Nucl. Phys.* **30**, 468 (1962).

²¹ R. W. Peelle, *Phys. Rev.* **105**, 1311 (1957).

²² Y. Nagahara, *J. Phys. Soc. Japan* **16**, 133 (1961).

investigated during this experiment. Measurements were made of $P_{2,eff}$ below 14 MeV relative to the known values of $P_{2,eff}$ above 14 MeV. This was done by measuring the left-right asymmetry under the same conditions of deuteron bombarding energy and reaction angle (i.e., the same P_1) for two different sets of foils in front of the carbon target. In this manner two new measurements of P_2 for $C^{12}(p,p)C^{12}$ were obtained. They are shown in Fig. 3.

Using the same technique, the polarization in proton-carbon scattering was also investigated at energies above 18 MeV. The results are: $P_2 = -0.25 \pm 0.08$ for a mean proton energy of 21.5 MeV and a target thickness of 1 MeV and $P_2 = -0.36 \pm 0.05$ for a mean proton energy of 23.5 MeV and a target thickness of 2 MeV.

2. Measurement of Foil Thickness

In order to obtain an internally consistent set of measurements, independent of uncertainties in the analyzing power of carbon, it was decided to use as far as possible the same thickness carbon target and the same incident proton energy. The nature of the $He^3(d,p)He^4$ reaction is such that the proton energy for a given deuteron energy varies considerably over the angular range investigated. By using different thicknesses of slowing-down foils it was possible to take most of the forward angle data with 17.9-MeV protons incident on either a 2- or a 3-MeV thick carbon target.

A scintillation counter was used to determine the thickness of foil necessary to slow down the protons to the desired energy. The counter was calibrated with $He^3(d,p)$ protons of known energy. The energy of the $He^3(d,p)$ protons was calculated relativistically and corrected for various small energy losses in the He^3 target and in the foils. The over-all uncertainty of the proton energy incident on the carbon target of the analyzer was ± 100 keV. The calibrated scintillation counter was also used to measure the thickness of the carbon targets. The uncertainty of the mean proton energy in the carbon analyzer leads to an uncertainty in the effective analyzing power of ± 0.01 or less.

3. Polarization Measurements

Angular distributions of proton polarization were measured at deuteron energies of 3, 4, 6, 8, 10, and 12 MeV. The angular range from 20° to 140° in the laboratory system was investigated in 20° intervals except at 8 MeV where measurements were made in 10° steps. In addition, 30° was always measured to observe the forward maximum in the polarization.

For each measurement, counts were collected with the analyzer set at a given angle to one side of the incident deuteron beam; then counts for an equal number of deuterons were collected with the analyzer on the other side. The gas target cell was rotated through 180° between right and left measurements since the cell window was obstructed for an extent of 70° .

TABLE I. Polarization P_1 of protons from the $He^3(d,p)He^4$ reaction.

E_d (MeV)	$\theta_{1,lab}$ (deg)	$\theta_{1,c.m.}$ (deg)	E_p (MeV)	E_2 (MeV)	$P_{2,eff}$	P_1	
3.0	20	22.5	19.98	16.4	-0.52	0.102±0.031	
	30	33.5	19.62	16.4	-0.52	0.010±0.034	
	40	44.7	19.14	16.4	-0.52	-0.011±0.035	
	60	66.0	17.91	16.3	-0.52	-0.346±0.039	
	80	87.0	16.52	14.8	-0.53	-0.266±0.043	
	100	106.0	15.16	14.0	-0.51	-0.217±0.052	
	120	126.8	13.99	13.0	-0.51	-0.024±0.050	
	140	144.5	13.10	12.4	-0.56	-0.176±0.086	
	4.00	20	22.7	21.16	16.9	-0.50	0.183±0.022
		30	34.0	20.72	16.9	-0.50	0.182±0.024
40		45.5	20.14	16.9	-0.50	0.235±0.026	
60		67.0	18.69	16.9	-0.50	-0.330±0.024	
80		87.7	17.04	15.0	-0.53	-0.458±0.028	
100		108.0	15.45	14.3	-0.52	-0.284±0.030	
120		127.0	14.09	13.1	-0.51	-0.276±0.038	
140		145.5	13.08	12.4	-0.56	-0.232±0.044	
6.00		20	23.2	23.37	16.9	-0.50	0.358±0.030
		30	34.8	22.80	16.4	-0.52	0.514±0.022
	40	46.2	22.04	16.4	-0.52	0.430±0.026	
	60	68.4	20.15	16.4	-0.52	-0.121±0.030	
	80	89.6	18.04	16.4	-0.52	-0.446±0.030	
	100	109.6	16.04	15.0	-0.53	-0.543±0.030	
	120	128.3	14.38	13.4	-0.51	-0.444±0.040	
	140	146.2	13.16	12.5	-0.56	-0.434±0.052	
	8.00	11	13.1	25.85	16.4	-0.52	0.015±0.027
		20	23.7	25.47	16.4	-0.52	0.408±0.022
30		35.5	24.77	16.4	-0.52	0.676±0.022	
40		47.0	23.85	16.4	-0.52	0.542±0.024	
50		58.2	22.75	16.4	-0.52	0.189±0.031	
60		69.4	21.55	16.4	-0.52	-0.002±0.026	
70		80.2	20.29	16.4	-0.52	-0.178±0.031	
80		90.7	19.02	16.4	-0.52	-0.379±0.032	
90		101.0	17.80	16.1	-0.53	-0.425±0.040	
100		110.7	16.66	14.8	-0.53	-0.493±0.024	
110	120.1	15.63	14.4	-0.52	-0.549±0.052		
120	129.4	14.72	13.7	-0.51	-0.658±0.046		
10.00	140	147.0	13.32	12.6	-0.56	-0.469±0.048	
	20	24.0	27.51	16.4	-0.52	0.393±0.028	
	30	35.9	26.68	16.4	-0.52	0.757±0.028	
	40	47.5	25.60	16.4	-0.52	0.572±0.030	
	60	70.4	22.91	16.4	-0.52	0.014±0.028	
	80	91.7	19.99	16.4	-0.52	-0.278±0.030	
	100	111.5	17.29	15.5	-0.53	-0.380±0.030	
	120	130.2	15.11	13.8	-0.52	-0.424±0.038	
	140	147.5	13.55	12.9	-0.56	-0.463±0.044	
	12.00	20	24.4	29.51	16.4	-0.52	0.303±0.034
30		36.4	28.56	16.4	-0.52	0.725±0.036	
40		48.1	27.31	16.4	-0.52	0.424±0.046	
60		71.0	24.25	16.4	-0.52	0.152±0.058	
80		92.5	20.95	16.4	-0.52	-0.062±0.052	
100		112.5	17.93	16.3	-0.52	-0.236±0.040	
120		131.0	15.51	14.1	-0.52	-0.313±0.040	
140		148.2	13.80	12.7	-0.54	-0.352±0.048	

Two ratios were obtained: LL/LR and RR/RL , where LL stands for the number of counts in the counter which detected two scatterings to the left, etc. The

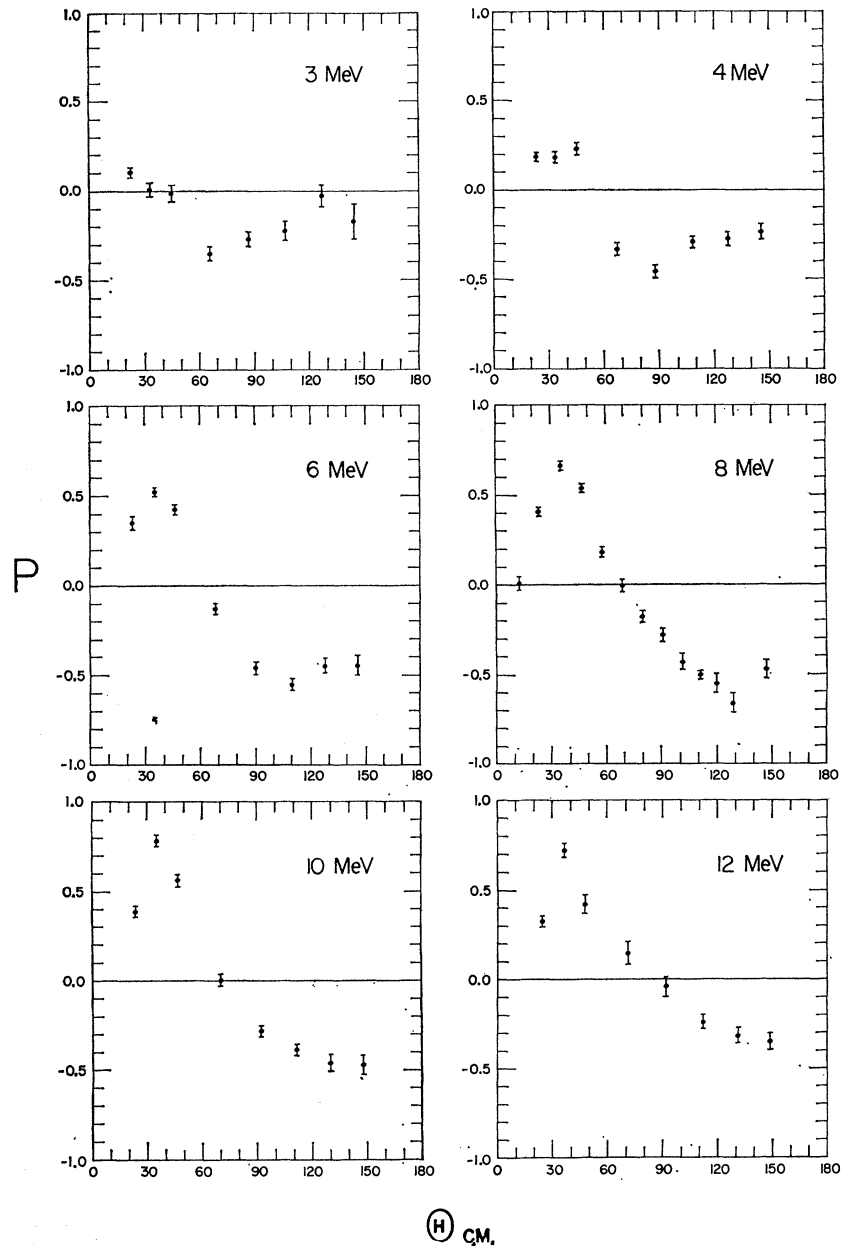


FIG. 5. Polarization of $\text{He}^3(d,p)$ protons as a function of reaction angle in the c.m. system for deuteron energies between 3 and 12 MeV.

geometric mean of these two ratios provides a ratio which is independent of the relative counter efficiency.²³

The coincidence circuit used for the 10- and 12-MeV measurements introduces possible counter asymmetries not present in the simpler electronic setup. Comparison of points taken at 8 MeV with and without the coincidence circuitry showed no evidence of a systematic difference.

4. Background Treatment

Figure 4 shows proton pulse-height spectra for different angles and deuteron energies. The energy of the

²³ I. Alexeff and W. Haeblerli, Nucl. Phys. 15, 609 (1960).

protons at the detector was similar throughout the measurements. The resolution of the photomultipliers was sufficient to separate the elastic and inelastic proton groups from carbon as shown in the 3-MeV spectrum. The inelastic group was usually masked by background as shown on the right-hand side of Fig. 4. For the spectra shown the coincidence counters were not used.

Background was measured by removing the carbon target and adding to the slowing-down foils a foil of a thickness equal to that of the target. Thus, the protons entering the region behind the target position had the same energy as during data runs. The geometry was such that the CsI detectors could "see" only about 1

cm of air which equals about 1 to 2% of the atomic thickness of the carbon target. However, in the pulse-height interval where the elastically scattered protons occurred, the number of background counts was seldom below 10% of the number of proton counts. When background was greater than 20%, runs measuring background were as long as data runs. Shorter runs were taken for backgrounds less than 20%.

The above background measurement would not eliminate counts caused by the interaction of scattered deuterons in the carbon analyzer. As an alternate way to measure the background, a target cell was filled with He^4 , so that there was no energetic (d,p) reaction, but still the same deuteron intensity from elastic scattering in the target foils as was present during the actual run. Runs were taken with and without the carbon target. In both cases the number of counts was found to be equal to that in the background runs taken in the manner described above with He^3 as first target. In addition, there was no change when the deuterons were stopped before reaching the carbon target.

The protons from deuteron breakup on He^3 were too low in energy to be counted.

5. False Asymmetries and Corrections

Differences in the counter efficiency are cancelled by interchanging the counters in the way described in the section on polarization measurements. In order to investigate possible errors in the measurements due to misalignment, the geometry of the scattering chamber and the analyzer was checked with an alignment telescope. The largest source of error is the uncertainty of ± 0.02 cm in the position of the He^3 target cell. The largest effect arises when the target cell is displaced from the axis of rotation of the analyzer in the direction parallel to the deuteron beam. In this case, P_1 can be in error by as much as ± 0.03 , depending on how rapidly the $\text{He}^3(d,p)$ cross section varies with angle. Errors from other possible misalignments are much smaller.

A correction was applied to the data (finite geometry correction) to compensate for errors due to the finite extent of the targets. These errors arise because in the first and the second target, cross section and polarization depends on angle and energy so that the observed asymmetry differs from the asymmetry that would have been obtained for the ray passing through the center of all apertures. The largest contribution to the correction comes from the variation of the $\text{He}^3(d,p)$ cross section σ_1 with reaction angle θ_1 , combined with the variation of the carbon cross section σ_2 with scattering angle θ_2 . However, the variation of the cross sections with energy; the variation of the polarization with angle and energy in both targets, and the variation of the solid angle of detection from different elements of first and second target were also considered in the calculations.

The amount by which P_1 was altered by the correc-

tion ranged from $+0.025$ to -0.015 , depending on reaction angle and deuteron energy. All calculations were performed by dividing the targets into a number of elements and by numerically adding the intensities of particles scattered into the detector. This was done for each particular combination of bombarding energy and reaction angle. The calculations were carried out in the median (horizontal) plane only and are accurate to about 30% of the value of the correction. The effect of the spread in azimuthal angle and the averaging of P_2 were already discussed in the section on analyzing power of carbon. For our particular geometry it was possible to treat these effects separately from the above calculations.

To have a rough experimental check whether there might be instrumental asymmetries beyond those covered by the calculations the reaction protons were in one case scattered from gold rather than carbon. Blanpied²⁴ measured a polarization of $+0.05 \pm 0.04$ for protons of a mean energy of 16.5 MeV scattered at a laboratory angle of 45° . In the present experiment protons from the $\text{He}^3(d,p)\text{He}^4$ reaction with a polarization of $+0.69 \pm 0.02$ and a mean energy of 17 MeV in the center of the gold were scattered by a 1.7-MeV thick gold target. The measured asymmetry led to an uncorrected polarization for scattering from gold of $+0.094 \pm 0.023$ and a corrected value of $P = +0.083 \pm 0.023$ in agreement with Blanpied's measurements.

IV. RESULTS

The polarization data obtained for the $\text{He}^3(d,p)\text{He}^4$ reaction are presented in Table I. Energies are given in the laboratory system. The first column is the deuteron energy at the center of the He^3 target. The next three columns list the reaction angle in the laboratory system, the reaction angle in the center-of-mass system and the laboratory energy of the reaction protons. The last three columns give the mean energy of the protons in the carbon analyzer, the effective analyzing power of carbon and the polarization of the $\text{He}^3(d,p)$ protons. The tabulated values of the polarization P_1 are corrected for instrumental effects in the manner described. The corrections are in most cases of the order of ± 0.01 . The corrections, the results of all individual runs and other details can be found in reference 15. The uncertainties of P_1 in Table I are the statistical uncertainties only and do not include the uncertainty of P_2 . From the work of Yamabe *et al.*¹⁷ and of Brockman¹⁹ one estimates that the relative error of $P_{2,\text{eff}}$ is between 5 and 10%.

The values of P_1 are plotted vs the center-of-mass reaction angle in Fig. 5. For all energies measured the polarization data are characterized by positive values at forward angles and negative values at larger angles. The polarization at forward angles becomes a pronounced maximum at the higher deuteron energies. The value of P_1 at this maximum is above $+0.50$ from

²⁴ W. A. Blanpied, Phys. Rev. **113**, 1099 (1959).

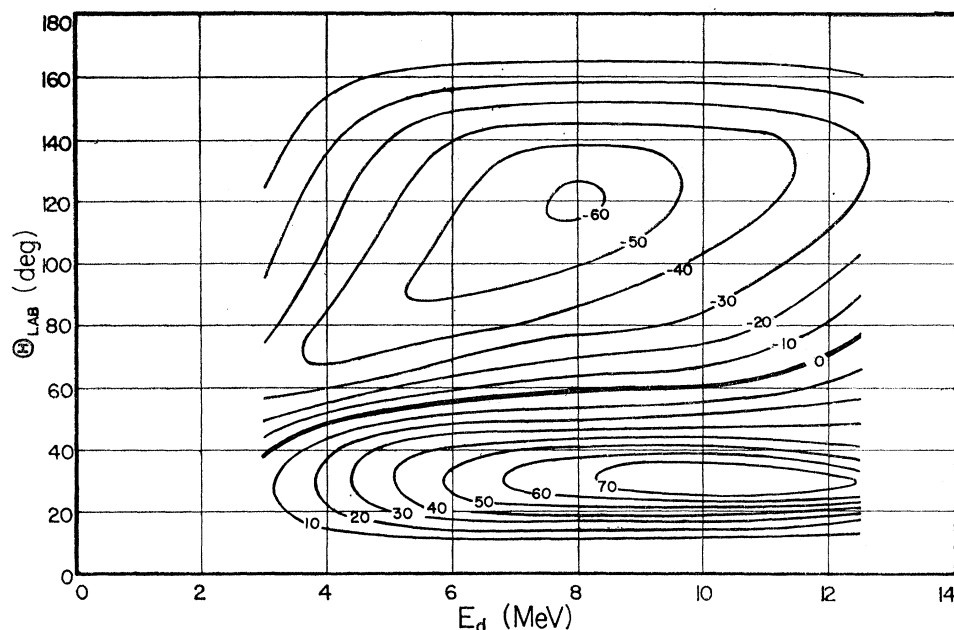


FIG. 6. Contour map of the polarization of protons from the $\text{He}^3(d,p)$ reaction. The lines of constant polarization were obtained from the data by free-hand interpolation between the measured points.

6 to 12 MeV. The highest value measured was $+0.76 \pm 0.03$ at $\theta_{\text{c.m.}} = 35.9^\circ$ for $E_d = 10$ MeV. The negative values of P_1 form a broad minimum which shifts slightly to larger angles with increasing deuteron energy. The most negative value measured is -0.66 ± 0.05 at $\theta_{\text{c.m.}} = 129.4^\circ$ for $E_d = 8$ MeV.

A contour map of the proton polarization vs laboratory angle and deuteron energy is shown in Fig. 6. To obtain this map, free-hand curves were drawn through the data; then points of equal polarization were plotted on the graph. Smooth contour lines connecting these points were drawn.

V. DISCUSSION

The shape of the angular dependence of polarization is similar throughout the energy range investigated. The angular dependence of the cross section for the $\text{He}^3(d,p)$ reaction varies only slowly with energy; however, there is a considerable change in the shape of the curve between 3 and 12 MeV. At the lower energies the cross section² has a single, shallow minimum near 100° , while at 12 MeV there is a pronounced forward peak, a secondary maximum at 65° , followed by another minimum and a rise to backward angles. It may be noted that the forward peak in polarization occurs within a few deg of the angle where the cross section has the first minimum. The negative peak in polarization occurs at a somewhat larger angle than does the second minimum in the differential cross section. A further parallel between cross section and polarization lies in the fact that with increasing energy the two minima in the cross section become more pronounced, as does the forward and backward peaking of the polarization.

At the higher bombarding energies the angular dis-

tribution for the $\text{He}^3(d,p)$ and $\text{T}(d,n)$ reaction cross section resembles the typical deuteron stripping pattern. A plane-wave calculation²⁵ assuming zero angular momentum transfer by the captured nucleon reproduces the general features of the angular distribution up to the second minimum. This treatment, however, always predicts zero polarization. Recently, Tobocman²⁶ made calculations using distorted-wave Born approximation. Optical-model potentials were used for the distortion of incident deuteron and outgoing proton wave. The deuteron energy was 12.3 MeV. When the potential parameters were adjusted to give a good fit to the measured scattering cross sections of deuterons on He^3 and of protons on He^4 , the resulting $\text{He}^3(d,p)$ angular distribution agreed only qualitatively with the observed cross sections. The amplitude of the first minimum and the second maximum relative to the forward peak is about right, but the peak occurs at too large an angle and the calculated cross section increases too much at back angles. The optical potentials contained a spin-orbit term. Such a term in at least one potential is mandatory, as in the special case of neutron capture into an s state there would otherwise be no polarization of the stripped proton. The calculated proton polarization was of the right order of magnitude, but the angular dependence bore no relation to the observed polarization.

Biedenharn and Satchler²⁷ suggested that in a stripping reaction which involves s -wave capture there

²⁵ S. T. Butler and J. L. Symonds, Phys. Rev. **83**, 858 (1951).

²⁶ W. Tobocman, in *Proceedings of the Rutherford Jubilee International Conference* (Heywood and Company, London, 1961), p. 465, and (private communication).

²⁷ L. C. Biedenharn and G. R. Satchler, Suppl. Helv. Phys. Acta **VI** (1961), p. 372.

might be a relation between cross section and polarization similar to the "derivative rule" of the optical model. This would require that the polarization changes sign at those angles where the derivative of the cross section with respect to angle is zero. The present data definitely contradict the proposed rule.

VI. CONCLUSIONS

The polarization of $\text{He}^3(d,p)$ protons was found to be remarkably high. Values as high as 0.76 were observed. While in elastic scattering of nucleons very large polarization is quite common, the peak polarization found here is higher than in any other reaction. This makes the $\text{He}^3(d,p)$ reaction an interesting source of polarized protons of relatively high energy. For deuteron energies from 7 to 12 MeV, the protons emitted at 30° have energies between 24 and 28.6 MeV and polarization of 0.6 or higher. At backward angles, protons of energy 14–16 MeV with somewhat lower polarization can also be obtained. An alternate way of producing polarized protons of energy above 20 MeV is by elastic scattering from He^4 . However, for proton energies approaching 30 MeV the polarization in $p\text{-He}^4$ scattering is not known very accurately. The cross section at the angle of large polarization²⁸ is not much larger than in the $\text{He}^3(d,p)$ reaction.

From the charge symmetry of nuclear forces one expects the $\text{He}^3(d,p)\text{He}^4$ and the $\text{T}(d,n)\text{He}^4$ reaction to behave in a similar way. The difference in Q value between the reactions is small and for bombarding energies above a few MeV the Coulomb effects are relatively unimportant. Stewart *et al.*,⁵ and Goldberg and LeBlanc⁶ found, indeed, that the cross section of the two reactions are practically identical for bombarding energies of 6 MeV and higher. It is, therefore, interesting to compare the polarization of the outgoing nucleons in the two reactions. Measurements have been carried out at Los Alamos⁹ and at Wisconsin¹⁰ of the polarization of $\text{T}(d,n)$ neutrons, using scattering from He^4 as analyzer. These measurements are difficult to interpret because the analyzing power of helium is not known accurately, particularly for the higher neutron energies. In order to arrive at an estimate of the analyzing power, Perkins and Simmons⁹ assumed that the $n\text{-He}^4$ phase shifts are equal to the $p\text{-He}^4$ phase shifts of

²⁸ J. L. Gammel and R. M. Thaler, Phys. Rev. **109**, 2041 (1958).

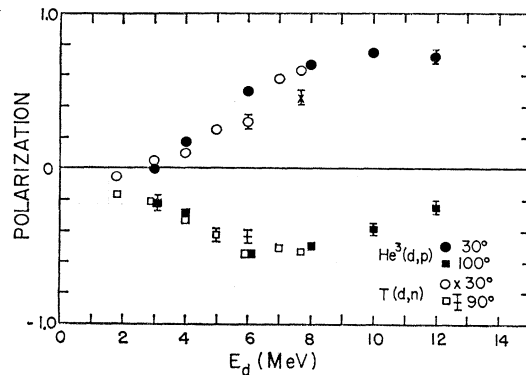


FIG. 7. Comparison of the polarization of the outgoing nucleons in the $\text{He}^3(d,p)\text{He}^4$ and the $\text{T}(d,n)\text{He}^4$ reaction. The neutron measurements are by Perkins and Simmons (reference 9) and Benenson *et al.*, (reference 10). The statistical errors of the measurements are comparable to the size of the dots, except where indicated.

Gammel and Thaler.²⁸ The resulting values of the neutron polarization in the $\text{T}(d,n)$ reaction for reaction angles of 30° and 90° are plotted in Fig. 7 and are compared to the proton polarization in the mirror reaction at angles of 30° and 100° . The agreement between proton and neutron results is very good. This is somewhat surprising, because the $n\text{-He}^4$ phase shift which were used are certainly inaccurate, since they give a poor fit to the $n\text{-He}^4$ angular distribution. Also shown in Fig. 7 are two measurements by Benenson, Walter, and May¹⁰ who obtained $n\text{-He}^4$ phase shifts by extrapolating Seagrave's curves²⁹ to higher energies. Their analyzing power differs only little from that of Perkins and Simmons although the phase shifts are quite different. So far it appears that whatever discrepancies there may be between the polarization measurements in the two mirror reactions they can be explained by the uncertainties of the analyzing power in the neutron experiments. This also applies to the very recent neutron polarization experiment of R. L. Walter *et al.*³⁰

ACKNOWLEDGMENTS

We should like to thank W. G. Weitkamp, R. A. Blue, and R. L. Douglas for their help in preparing the equipment and in taking the data.

²⁹ J. D. Seagrave, Phys. Rev. **92**, 1222 (1953).

³⁰ R. L. Walter, W. Benenson, T. H. May and A. S. Mahajan, Bull. Am. Phys. Soc. **7**, 268 (1962); and R. L. Walter (private communication).